Fgf signals from a novel signaling center determine axial patterning of the prospective neural retina

Alexander Picker* and Michael Brand

University of Technology, Department of Genetics, c/o Max Planck Institute of Molecular Cell Biology and Genetics, Pfotenhauer Strasse 108, 01307 Dresden, Germany
*Author for correspondence (e-mail: picker@mpi-cbg.de)

Accepted 2 September 2005

Development 132, 4951-4962
Published by The Company of Biologists 2005
doi:10.1242/dev.02071

Summary

Axial eye patterning determines the positional code of retinal ganglion cells (RGCs), which is crucial for their topographic projection to the midbrain. Several asymmetrically expressed determinants of retinal patterning are known, but it is unclear how axial polarity is first established. We find that Fgf signals, including Fgf8, determine retinal patterning along the nasotemporal (NT) axis during early zebrafish embryogenesis: Fgf8 induces nasal and/or suppresses temporal retinal cell fates; and inhibition of all Fgf-receptor signaling leads to complete retinal temporalization and concomitant loss of all nasal fates. Misprojections of RGCs with Fgf-dependent alterations in retinal patterning to the midbrain demonstrate the importance of this early patterning process for late topographic map formation. The crucial period of Fgf-dependent patterning is at the onset of eye morphogenesis. Fgf8 expression, the restricted temporal requirement for Fgf-receptor signaling and target gene expression at this stage suggests that the telencephalic primordium is the source of Fgf8 and acts as novel signaling center for non-autonomous axial patterning of the prospective neural retina.

Key words: Eye development, Axial patterning, Nasal, Temporal, Fgf, Fgf8, Efn, Eph, Zebrafish, *Danio rerio*

Introduction

The retinotopic organization of the midbrain optic tectum in fish, amphibians and birds, or superior colliculus in mammals is a highly precise representation of positional cell identities in the retina, because, according to the position of their somata in the eye, retinal ganglion cell (RGC) axons project topographically to the tectum. As a result, the nasal-temporal (NT) and dorsal-ventral (DV) axes of the retina map inversely to the anterior-posterior (AP) and DV axes of the tectum (McLaughlin et al., 2003). Molecularly, topographic mapping of RGC axons is controlled by axon guidance cues of the Efn (Ephrin) class, which mediate axon repulsion by binding Eph tyrosine kinase receptors. Complementary, axial gradients of Eph-receptors on RGCs in the retina and Efn-ligands on the tectum direct this process (Drescher et al., 1995; Cheng et al., 1995; Flanagan and Vanderhaeghen, 1998). The topology of the retinotectal map requires precedent axial patterning to define positional cell identities and to restrict the expression of guidance cues in the retina and tectum. For the tectal target field, the midbrain-hindbrain boundary (MHB), located posterior to the tectum, controls patterning along the anterior-posterior (AP) axis during embryonic development. The secreted growth factor Fgf8 is expressed at the MHB, asymmetric to the tectum, and has a 'posteriorizing' influence on early midbrain polarity and later retinotopic organization of the tectum (Crossley et al., 1996; Itasaki and Nakamura, 1996; Friedman and O'Leary, 1996; Logan et al., 1996; Reifers et al., 1998; Martinez et al., 1999; Picker et al., 1999; Nakamura and Sugiyama, 2004).

The anatomical stages of vertebrate eye development are well described (Chow and Lang, 2001; Chuang and Raymond, 2002). In the zebrafish, eye morphogenesis commences with the lateral evagination of the optic vesicle from the diencephalic neural keel at 5- to 6-somite stage (Schmitt and Dowling, 1994). But it is not well understood how early eye morphogenesis relates to axial patterning of the prospective neural retina and how this influences topography of the retinotectal map (Peters, 2002). DV eye patterning involves bone morphogenetic protein 4 (BMP4), which is expressed in the dorsal eye and leads to upregulation of the dorsal T-box transcription factor Tbx5 and to downregulation of the ventral homeodomain transcription factors Vax and Pax2 upon misexpression (Koshiba-Takeuchi et al., 2000; Sasagawa et al., 2002). BMP loss/inhibition results in ventralization of the retina (Sakuta et al., 2001; Sasagawa et al., 2002; Murali et al., 2005). Vax genes are required for ventral retina development and to delineate optic stalk from retinal territories; the latter through a midline-derived Hedgehog (Hh) signal (Schulte et al., 1999; Barbieri et al., 1999; Mui et al., 2002; Take-uchi et al., 2003). Asymmetric distribution of retinoic acid (RA) has also been implicated in DV eye patterning (Hyatt et al., 1992; Kastner et al., 1994; Marsh-Armstrong et al., 1994; Hyatt et al., 1996). A recent study suggested that RA and Fgfs can ventralize the eye by collaborating with Hh, but the exact temporal requirement for these factors remains largely unclear

(Lupo et al., 2005). In the chick, retinal DV polarity is gradually determined between the 8- and 14-somite stage (Uemonsa et al., 2002).

By contrast, retinal patterning along the NT axis is only poorly understood. The forkhead transcription factors Foxg1 (BF1) and Foxd1 (BF2) display restricted and complementary expression along the retinal NT axis and cause RGC axon misprojections upon ectopic expression (Hatini et al., 1994; Yuasa et al., 1996). Two transcription factors, sensory organ homeobox (SOHo) and *Gallus gallus* homeobox 6 (GH6) are expressed in the nasal half of the eye, and cause RGC axon misprojections upon ectopic expression and downregulation of temporal expression of Epha3a (Deitcher et al., 1994; Schulte and Cepko, 2000; Stadler and Solursh, 1994). Foxg1 can induce ectopic nasal gene expression (SOHo, GH6, Efna5, Efna2) and suppress temporal gene expression (Epha3, Foxd1) upon misexpression in the temporal retina (Takahashi et al., 2003). Despite increasing knowledge about late DV and NT axial restriction of gene expression in the retina, it is largely unknown when and through which factors these patterns are established (McLaughlin et al., 2003). Importantly, the currently known factors that regulate NT eye patterning are themselves already expressed asymmetrically. Fgf signals have been implicated in various aspects of eye development, including the segregation of neural from pigmented retina, lens induction and differentiation, retinal cell fate specification, photoreceptor survival, RGC axon outgrowth and axon guidance, and are thus good candidates to play a role in axial eye patterning (Russell, 2003; Yang, 2004). Furthermore, Fgf-dependent differentiation of the retina is mediated by a combined Fgf8/Fgf3 signal (McCabe et al., 1999; Martinez-Morales et al., 2005).

We had previously shown that RGCs from *fgf8*-mutant eyes form topographically incorrect axon projections on wild-type tecta, suggesting a role for Fgf8 in axial patterning of the retina (Picker et al., 1999). Here, we analyze the exact temporal and spatial requirement for Fgf signaling during axial patterning of the retina. Gene expression along the NT and DV axis of the retina in the *fgf8*-mutant *acerebellar* (*ace*), upon pharmacological inhibition of Fgf-receptor (Fgfr) signaling and upon ectopic Fgf8 expression shows that Fgf8 together with other Fgf proteins determines the NT axis. The temporal requirement for Fgfs is tightly restricted to the onset of eye morphogenesis between the 5- and 10-somite stage. Heterotopic eye transplantations show that this early patterning phase is sufficient to drive subsequent autonomous NT eye patterning. We also show that the early, Fgf-dependent positional code of cells along the NT axis of the eye determines later topographic mapping of RGC axons along the anterior-posterior axis of the midbrain tectum. The developmental timing of (1) *fgf8* expression and its patterning activity, (2) of the requirement for Fgfr signaling and (3) of activation of the Fgf-target gene *spry4* in the diencephalon and eye suggest that the telencephalon acts as extrinsic Fgf-source and thus is a novel signaling center for retinal patterning.

Materials and methods

Fish maintenance

Fish were maintained at 28°C on a 14 hour light/10 hour dark cycle (Westerfield, 2000). Embryos were staged according to (Kimmel et al., 1995) or in hours post-fertilization at 28°C for 24 hours old or older embryos. The data we present in this study were obtained from analysis of AB or TL wild-type fish and of homozygous *acerebellar*^{ti282a} (*ace*) embryos (Brand et al., 1996). Molecular analysis indicates that *ace*^{ti282a} is a complete loss-of-function allele (Reifers et al., 1998) (M.B., unpublished).

Whole-mount in situ hybridization, immunocytochemistry and cell death analysis

Whole-mount mRNA in situ hybridization were carried out as described (Reifers et al., 1998). Digoxigenin-labeled probes were prepared from linearized templates using an RNA labeling and detection kit (Roche). Receptor alkaline phosphatase staining with the chick for Epha3-AP fusion protein was carried out as previously described (Cheng and Flanagan, 1994; Brennan et al., 1997). Apoptotic cells were detected by an in-situ nick-end labeling procedure using a commercial kit (Roche). Acridine Orange (AO, Molecular Probes) was used at a concentration of 2 μg/ml to stain live embryos (Brand et al., 1996).

Gene expression intensity profiling

For intensity profiling of retinal gene expression, sets of 8-bit grayscale images of dissected, flat mounted eyes where captured after in situ hybridization as described above. Images where subsequently imported into the ImageJ 1.32j (http://rsb.info.nih.gov/ij/) image analysis software. Using the 'Analyze>Plot Profile' option intensity profiles along radial trajectories were captured and further analyzed with Microsoft Excel. Comparisons of gene expression in wild-type and mutant where performed on embryos from the same egg lay and were stained, imaged and analyzed under identical conditions.

Fgfr-inhibitor treatment

The Fgf-receptor signaling inhibitor SU5402 (Calbiochem) (Mohammadi et al., 1997) was diluted into 10 mM stocks in DMSO and added to E3 medium at a working concentration of 5 μM, followed by repeated washing in excess medium. Control embryos were treated in 0.05% DMSO (Reifers et al., 2000).

Tissue transplantations, bead implantations and RGC axon labeling

Optic vesicle transplantation and anterograde RGC labeling was carried out as described before on the same side of donor and host embryo (Picker et al., 1999). Fgf8-protein beads were prepared by overnight incubation of heparin-coated acrylic beads (Sigma) or 45 μm polystyrene beads (Polysciences) in a 250 μg/ml solution of recombinant zebrafish Fgf8 protein in PBS. Before implantation, beads were rinsed three times for 10 minutes in PBS. Control beads were loaded with 250 μg/ml BSA.

Results

Fgf signaling regulates NT patterning of the prospective neural retina

Various Fgfs are expressed in and around the forming eye from neural plate stages of embryogenesis onwards. We therefore designed experiments to determine if Fgf signaling plays a role in patterning of the prospective retina along the nasal-temporal (NT) and dorsal-ventral (DV) axis. Our initial approach was to alter levels of Fgf signaling by (1) implantation of Fgf8-protein-coated beads to increase signaling; and (2) treatment of embryos with the pharmacological Fgf receptor (Fgfr) inhibitor SU5402 to block signaling during early eye development and to study the response of genes with restricted expression along the retinal axes at the 28 hour stage. Of the genes that are restrictively expressed along the NT axis we analyzed the forkhead-transcription factor *foxg1* (*BF1*), which

is expressed in the nasal half of the prospective retina, and two axon guidance molecules of the Eph/Efna class – the *efna5a* ligand, which is expressed nasally, and the *epha4b* receptor, which is expressed temporally. Of the genes that are discretely expressed along the DV axis, we analyzed the T-box transcription factor *tbx5* as dorsal marker and the homeobox gene *vax2* as ventral marker.

In wild-type embryos at 28 hours, expression of *efna5a* is confined to cells in the nasal half and *epha4b* to cells in the temporal half of the prospective retina (Fig. 1B,E). Fgf8-bead implantation between the 5- and 7-somite somite stage close to the retina (Fig. 1A,D) leads to a strong 'temporal shift' in retinal gene expression: temporal expansion of the nasally expressed gene *efna5a* (*n*=7/7) and complementary repression of the temporally expressed *epha4b* (*n*=8/8) (Fig. 1C,F). Similar to Fgf8 beads, transplantation of cells from the telencephalic *fgf8* expression domain at the 5-somite stage (see Fig. 5A,B) into the optic vesicle can repress temporal *epha4b* expression (*n*=3/4) showing that they can act as source of the patterning activity (Fig. 1G-I). Implantation of Fgf8-soaked beads after the 5- to 7-somite stage does not alter NT patterning (*n*=17/17). This Fgf8-misexpression phenotype strikingly resembles the phenotype of the *aussicht* (*aus*) mutant, where Fgf8 expression is generally increased (Heisenberg et al., 1999).

To determine the exact timing of the requirement for Fgf8 in NT eye patterning, we applied the pharmacological Fgfr inhibitor SU5402 to wild-type embryos at discrete developmental intervals between the 1- and 15-somite stage, and studied retinal gene expression at the 28 hour stage (Mohammadi et al., 1997; Reifers et al., 2000; Raible and Brand, 2001). Blocking Fgfr signaling induces a complete 'nasal shift' of retinal NT polarity: in wild-type control embryos, the expression of *epha4b* is strictly confined to the temporal half of the retina at the 28 hour stage (Fig. 2A). After treatment between the 1- and 5-somite stage, the expression of *epha4b* partially expands into the nasal retina (Fig. 2B). Treatment between the 3- and 8-somite stage and the 5- and 10-somite stage leads to an apparently complete expansion of *epha4b* throughout the retina (Fig. 2C,D). Complementary to this expansion, the nasal expression domains of *efna5a* (Fig. 2G, compare with Fig. 3C for wild-type expression) and *foxg1* (Fig. 2F, compare with Fig. 3A for wild-type expression) are completely lost. The dorsal expression domain of *tbx5* is not affected in its DV extent but shifts position nasally (Fig. 2H, compare with Fig. 3G). The ventral domain of *vax2* expression is unaffected (Fig. 2I, compare to Fig. 3I). Treatment beyond the 10-somite stage has no influence on *epha4b* expression (Fig. 2E) and retinal patterning in general.

To qualitatively analyze even subtle shifts in gene expression, we quantified RNA expression levels in the eye in flat-mount preparations by image analysis after in situ hybridization (Fig. 2J,K). For this purpose, linear intensity profiles were captured along a defined trajectory through the eye on digital image sets. As it has been noticed that regulatory genes in the eye are differentially expressed not only along a

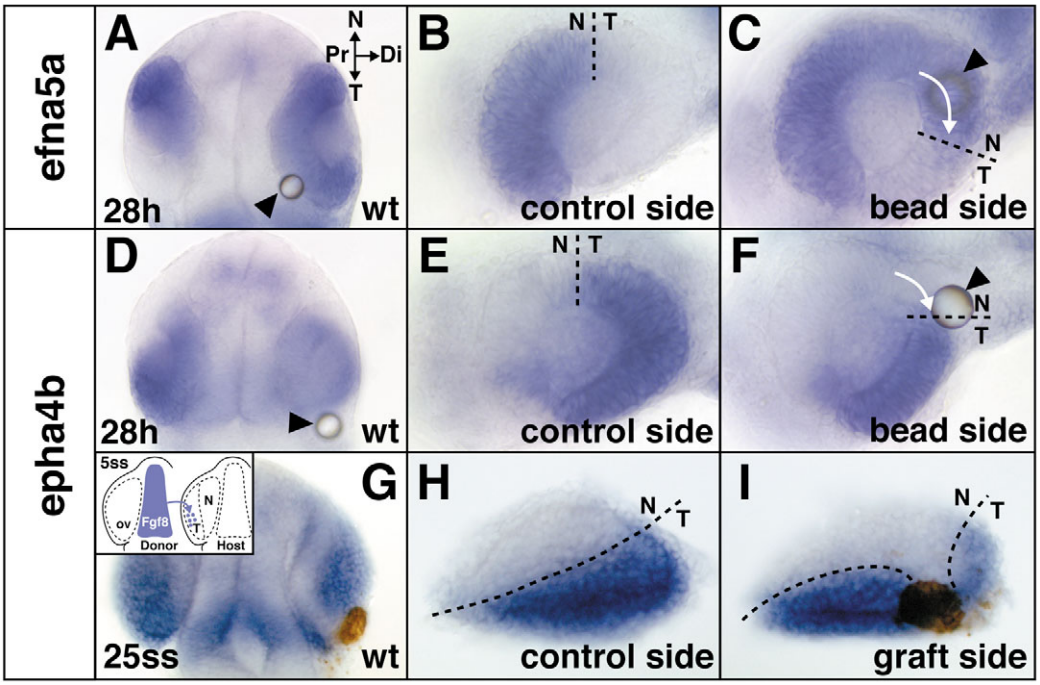

Fig. 1. Temporal shifts in retinal patterning induced by ectopic Fgf8. (A-F) Shifts in retinal NT gene expression at the 28 hour stage after Fgf8-bead implantation at the 5-somite stage into wild-type (wt) embryos: expansion of the nasal marker *efna5a* (A,C) and reduction of the temporal marker *epha4b* (D,F) compared with control side of the same embryos (B,E). (G-I) Reduction of temporal *epha4b* expression in a wild-type embryo at the 25-somite stage after ectopic transplantation of cells from the telencephalic Fgf8-domain into the optic vesicle (ov, brown staining) at the 5-somite stage (I) compared with control side of the same embryo (H) (see inset in G for grafting schematic). Arrows indicate directionality of expansion/reduction. Location of the bead is indicated by arrowheads. (A,D,G) Dorsal views with anterior towards the top, orientation as indicated in A; (B,C,E,F,H,I) flat-mounts of dissected eyes. (C,F,I) Digitally inverted images. N, nasal; T, temporal; Pr, proximal; Di, distal. Dashed lines indicate the retinal NT boundary.

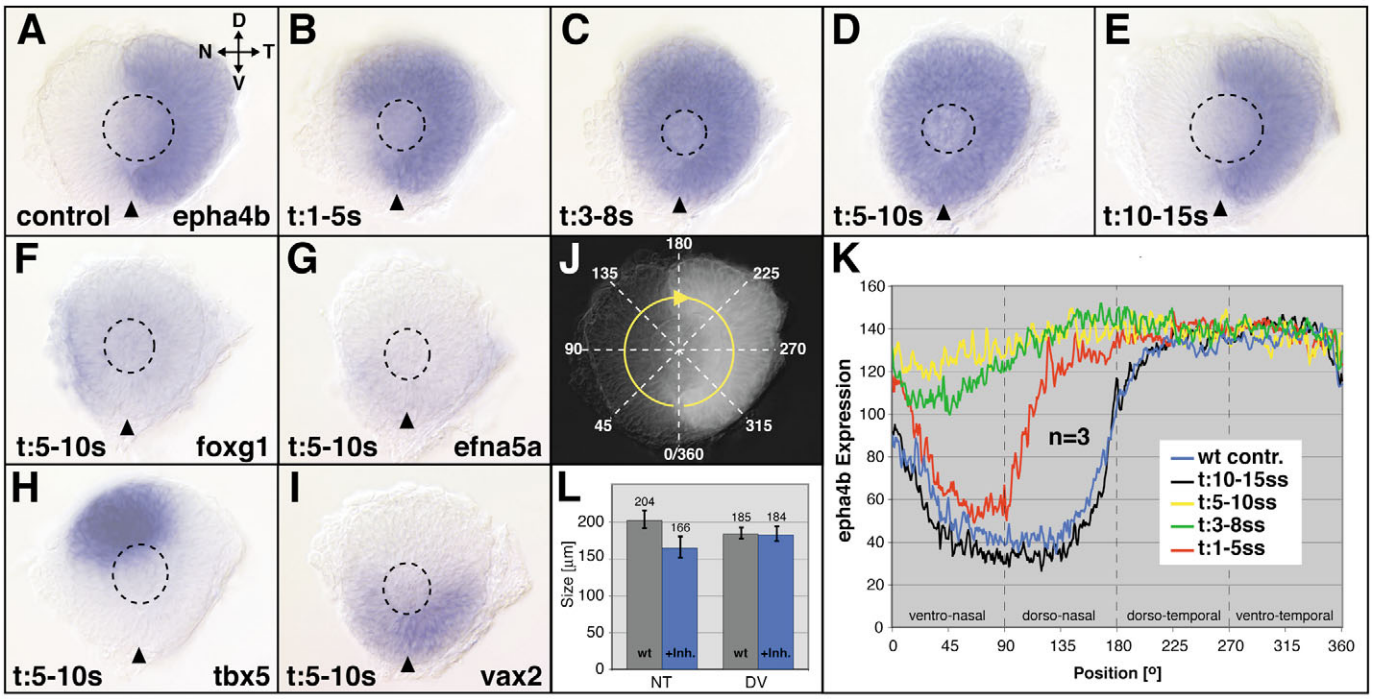

Fig. 2. Nasal shifts in retinal patterning after Fgf-receptor (Fgfr) inhibition. (A-E) *epha4b* gene expression at the 28 hour stage after Fgfr inhibitor treatment between the 1- and 5-somite stage results in a partial expansion of *epha4b* from the temporal half into the nasal retina (B). Treatment between the 3- and 8-somite stage (C), and 5- and 10-somite stage (D) induces expansion of *epha4b* expression throughout the retina. Treatment between the 10- and 15-somite stage has no effect on *epha4b* expression (E). Mock-treated control in A. Nasal expression of *foxg1* (F) and *efna5a* (G) is absent after treatment between the 5- and 10-somite stage (compare with Fig. 3A,C). (H) Dorsal *tbx5* expression is shifted nasally (compare with Fig. 3G), *vax2* expression is not altered (I) (compare with Fig. 3I). (K) Gene expression intensity profiling of *epha4b* in the retina at 28 hours along a clockwise 360° profiling trajectory (J) after Fgfr-inhibitor treatment (mean values, *n*=3 eyes): comparison of *epha4b* expression gradients shows the peak in the requirement for Fgfr signaling in retinal NT patterning during the 5- and 10-somite stage (yellow). Treatment periods are color-coded as indicated. Axial positions (in radial degrees of a circle; 0°/360°=ventromedial retina) along the profiling trajectory (*x*-axis) are plotted against the expression level (mean values of three eyes) in gray values on an 8-bit scale (*y*-axis). (L) Eye size after Fgfr-inhibitor-treatment along the NT and DV axis compared with wild-type control eyes. Sizes (μm) are mean values (*n*=9). Images are flat-mounts of dissected eyes, orientation as indicated in A. Dashed outlines indicate the position of the lens. Arrowheads indicate the ventralmost position of the eye marked by the choroid fissure. D, dorsal; V, ventral; N, nasal; T, temporal.

single axis (McLaughlin et al., 2003) 'straight-line intensity profiling' along the canonical NT and DV axes would not capture all changes in gene expression. We therefore applied a 'radial profiling scheme' along a clockwise 360° trajectory through the eye (Fig. 2J). Intensity profiling of *epha4b* gene expression (mean values, *n*=3 eyes) reveals that treatment between the 1- and 5-somite stage leads to partial nasal shift of the *epha4b* expression gradient into the dorsal retina, complementary to the partial temporal shift upon ectopic Fgf8 expression (compare with Fig. 1C,F). After treatment between the 3- and 8-somite stage, a remnant gradient is still detectable, whereas treatment between the 5- and 10-somite stage eliminates the gradient completely (Fig. 2K). Apart from a small size reduction along the NT axis (*n*=9) and of the lens, eyes of inhibitor treated embryos have no obvious morphological defects (Fig. 2L).

Thus, increased Fgf signaling through local misexpression of Fgf8 between the 5- and 7-somite stage can induce a 'temporal shift' in retinal patterning, suggesting that Fgf8 itself is the patterning activity. Blocking Fgf signaling through Fgfr-inhibitor treatment conversely induces a 'nasal shift'. In contrast to the partial shift in NT patterning after Fgf8-bead implantation, the temporalization after Fgfr-inhibitor treatment is complete. The requirement for Fgf signaling peaks between the 5- and 10-somite stage, the same period when ectopic Fgf8 protein can induce NT patterning shifts. Telencephalic, Fgf8-expressing cells can repress temporal cell fates upon ectopic transplantation into the eye in the same developmental interval, which suggests that the telencephalon – the only anterior expression domain of *fgf8* at that time (see Fig. 5A,B) – is the source of Fgf8.

Fgf8 is part of a combinatorial Fgf signal for retinal patterning

To determine if *fgf8* is required for retinal patterning, we analyzed gene expression in *fgf8*-mutant *acerebellar* (*ace*) embryos at 28 hours of development by in situ hybridization (Fig. 3A-J).

In wild-type embryos, *foxg1* is expressed in the nasal half of the eye, including the complete ventronasal but only the ventral part of the dorsonasal retinal quadrant. In *ace* mutant embryos, *foxg1* expression in the ventronasal quadrant is unaffected but appears reduced in the dorsonasal retina (Fig. 3A,B). Intensity profiling, along a clockwise 180° trajectory through the dorsal eye (mean values, *n*=8 eyes/gene) (Fig. 3L), reveals that *foxg1* is expressed in a nasal-to-temporal

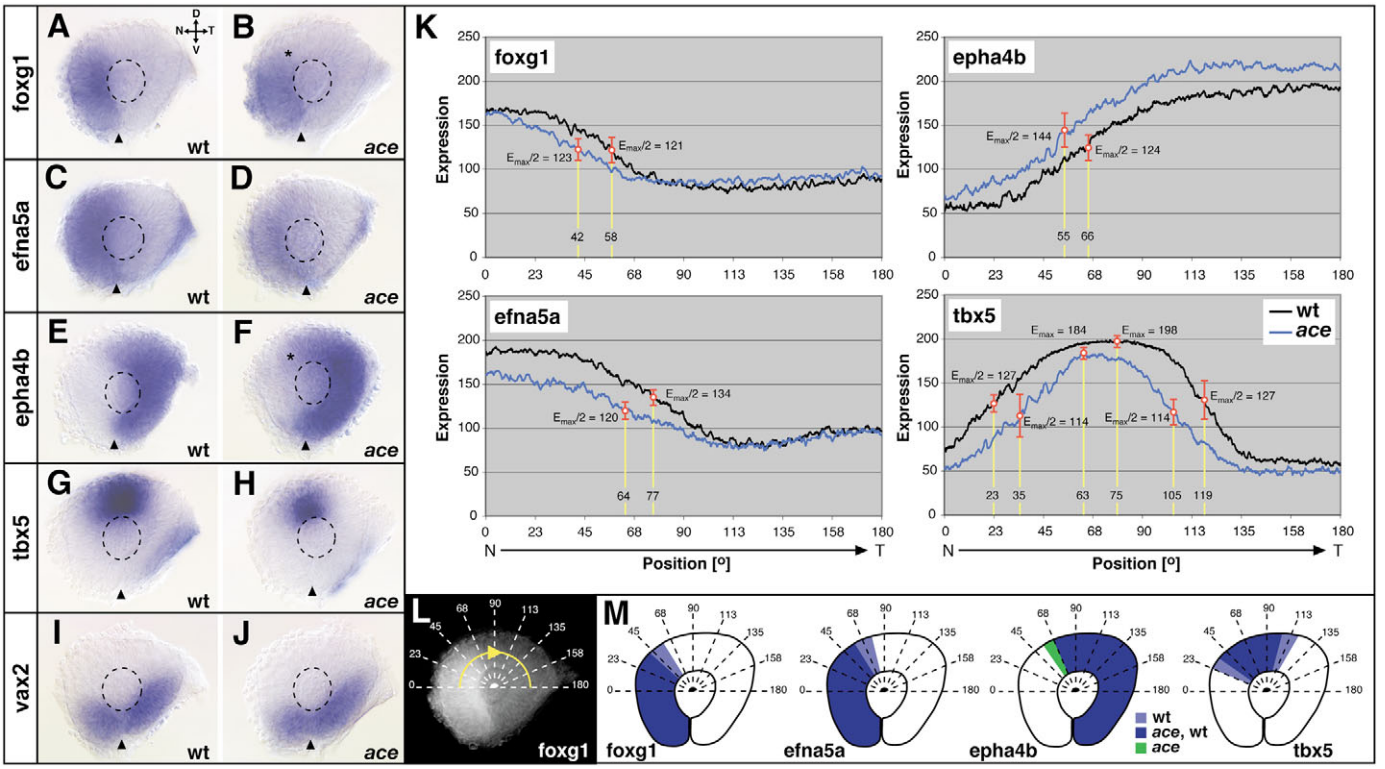

Fig. 3. Nasal shifts in retinal patterning in *fgf8*-mutant *ace* embryos. (A-J) In situ hybridizations of wild-type and the *fgf8*-mutant *acerebellar* (*ace*) at 28 hours. Expression of *foxg1* is confined to the nasal retina but not expressed to the dorsal-most point in wild type (A) and reduced (asterisk) in the dorsonasal retina of *ace* mutants (B). Expression of *efna5a* covers the complete nasal retina in wild type (C) and is reduced overall in *ace* (D). Expression of *epha4b* is confined to the temporal retinal half of the wild type (E), is fully complementary to *efna5a* (C) and expands (asterisk) into the nasal retina in *ace* (F). Expression of *tbx5* is confined to the dorsomedial retina in the wild type (G) and reduced in its nasotemporal extent in *ace* (H). *vax2* is expressed in the ventral retina of the wild type (I) and unaffected in *ace* (J). (K-M) Intensity profiling of gene expression in the dorsal retina along a clockwise 180° trajectory (L). (K) Graphs of intensity profiles of wild type (black) and *ace* mutant (blue) retinae (mean values, n=8 eyes/gene): in the wild type, *foxg1* is expressed in a nasal-to-temporal decreasing gradient, which is shifted nasally in *ace* (16° offset in $E_{max}/2$). The nasal-to-temporal decreasing gradient of *efna5a* in the wild type is reduced overall and shifted nasally in *ace* (13° offset in $E_{max}/2$). The nasal-to-temporal increasing gradient of *epha4b* in the wild type is nasally shifted owing to upregulation of expression in *ace* (11° offset in $E_{max}/2$). The bell-shaped expression gradient of *tbx5* in the wild type is steeper in *ace* (13° offset in $E_{max}/2$ nasally and temporally) and the central peak of *tbx5* expression, $-E_{max}$ value-, is shifted nasally in the mutant (radial offset=12°). Axial positions in radial degrees along the profiling trajectory (x-axis) are plotted against the expression level in gray values on an 8-bit scale (y-axis). Drop-lines in K indicate points of half-maximal $E_{max}/2$ and maximal E_{max} expression; corresponding expression values, radial positions and representative standard deviations (error bars) are indicated. (M) Schematic representations of gene expression domains. Boundaries are deduced from $E_{max}/2$ values in K. Extent of expression domains in wild type and *ace* are color-coded as indicated. Orientation of eyes as indicated in A. D, dorsal, V, ventral, N, nasal, T, temporal. Broken outlines indicate the lens. Arrowheads indicate the ventralmost position of the eye.

decreasing gradient, which is flattened in the dorsonasal retinal segment in the *ace* mutant, but reaches the same maximum and minimum expression levels (Fig. 3K). Similar to *foxg1*, *efna5a* is expressed in the nasal half of the wild-type retina; however, *efna5a* is also expressed in the complete dorsonasal quadrant. Thus, *foxg1* expression is nested within the *efna5a* expression domain. In *ace* mutant embryos, *efna5a* expression is overall strongly reduced (Fig. 3C,D). This leads to a global flattening of the nasal-to-temporal decreasing *efna5a* expression gradient in the mutant (Fig. 3K). In the wild type, *epha4b* is expressed throughout the temporal retina, complementary to *efna5a*. In *ace*, the *epha4b* expression domain expands into the dorsonasal retinal quadrant (Fig. 3E,F). As a result, the nasal-to-temporal increasing *epha4b* gradient is shifted in the *ace* mutant, indicating a global upregulation of expression (Fig. 3K). In the wild type, *tbx5* is expressed in the dorsomedial retina. In *ace* mutant embryos, the NT extent of *tbx5* appears reduced and shifted nasally (Fig. 3G,H). *Tb5x* is expressed in a bell-shaped gradient, which is centered on the dorsalmost point of the retina and bilaterally fades out into the dorsonasal and dorsotemporal quadrants. In the *ace* mutant, this bell-shaped gradient is flattened, indicating a global reduction in gene expression (Fig. 3K). In the wild type, *vax2* is expressed in the ventral retina. The expression domain covers two spatially distinct sub-domains: one in the ventronasal quadrant and one in the ventrotemporal quadrant, with the latter extending further dorsally than the other. The medial part of the ventral retina only weakly expresses *vax2*. In the *ace* mutant, *vax2* expression is unaffected (Fig. 3I,J). In sections along the canonical medial DV axis through the retina, we could not detect any differences between wild type and mutant (data not shown).

We used the intensity profiles to define the radial positions, where gene expression reaches half-maximal intensity values, $E_{max}/2$ (Fig. 3K). We defined this position as 'gene expression boundary'. Comparison between wild type and *ace* mutant eyes reveals that the position of the thus defined dorsal NT gene expression boundary undergoes a 'nasal shift' for *foxg1* (radial offset=16°), *efna5a* (radial offset=13°) and *epha4b* (radial offset=11°). The two lateral gene expression boundaries of *tbx5* both shift towards the dorsomedial eye (radial offset, nasal=12°, radial offset, temporal=14°), but importantly the central peak of *tbx5* expression, E_{max} value, is shifted nasally in the mutant (radial offset=12°). Schematic plotting on the basis of these boundary positions faithfully reproduces the gene expression patterns determined by microscopic imaging (compare schematics in Fig. 3M with Fig. 3A-J).

As described above, we found that ectopic Fgf8 protein cannot induce NT patterning shifts beyond the 10-somite stage. Nevertheless, late implanted beads are capable of rescuing the *ace* mutant eye phenotype: an Epha3-alkaline-phosphatase fusion protein detects Efna-ligand protein in the nasal half of the retina of wild-type embryos (Fig. 4A). The expression of Efna ligands is strongly reduced in *ace* mutant eyes, and rescued after bead implantation into the forebrain at the 10-somite stage (*n*=10/10) (Fig. 4C,D). Bead implantations into both wild type and *ace* mutants at this stage lead to ectopic expression of Efna ligands in the ventralmost region of the nasal retina, but do not induce nasal gene expression in the temporal retina (Fig. 4B,D).

One scenario that could explain the observed NT patterning shifts is the selective loss of the nasal and concomitant expansion of temporal retinal fates in *ace* and Fgfr-inhibitor-treated embryos. We therefore studied cell death during eye development in these embryos. Although we find a general increase in cell death in the eyes of *ace* and Fgfr-inhibitor treated embryos, this effect is not significant before the 20-somite stage. Likewise we do not observe a bias of cell death in *ace* and Fgfr-inhibitor treated embryos to the proximal, future nasal half of the eye (see Fig. S1 in the supplementary material). We therefore exclude the possibility that local cell death is the cause of the alterations in retinal NT patterning upon loss of Fgf signaling.

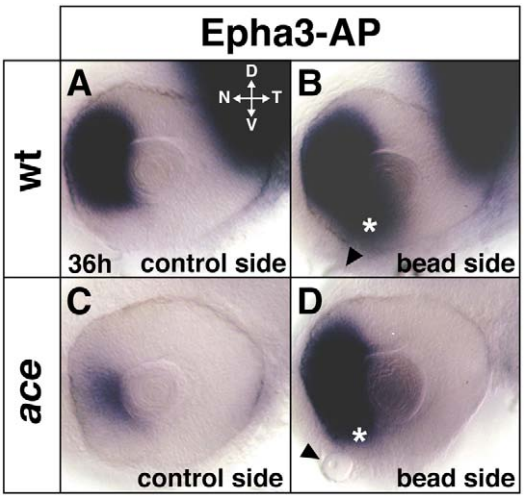

Fig. 4. Rescue of retinal patterning in the *ace* mutant by Fgf8-soaked beads. In 36-hour embryos, alkaline-phosphatase-tagged Epha3 protein detects nasal expression of Efna-ligands in the wild type (A), which is reduced in *ace* (C) and rescued after Fgf8-bead implantation at the 10-somite stage into the forebrain (D). Bead implantation also induces ectopic Efna-ligand expression in the ventronasal retina (asterisks in B,D). The sites of the beads are indicated by arrowheads. Images are flat-mounts of dissected eyes, orientation as indicated in A. (B,D) Digitally inverted images. D, dorsal; V, ventral; N, nasal; T, temporal.

We find that the lack of *fgf8* in the *ace* mutant causes a partial nasal shift of positional identities in the retina: expansion of temporal gene expression (*epha4b*) at the expense of nasal gene expression (*foxg1*, *efna5a*). Patterning along the DV axis (*tbx5*, *vax2*) appears unaffected. Fgf8 is able to rescue the *ace* mutant eye phenotype beyond the 5- to 7-somite stage, but without shifting NT patterning beyond its range in wild-type embryos. The observations in the genetic loss-of-function situation are consistent with the complete nasal shift after Fgfr-inhibitor treatment, and the temporal shift upon Fgf8 misexpression. Since the nasal shift in the *ace* mutant is partial compared with the phenotype after Fgfr-inhibitor treatment, we conclude that at least one other Fgf signal together with Fgf8 determines NT retinal patterning.

Early Fgf8 and Fgf-target expression suggests the telencephalon as signaling center for axial retinal patterning

Fgfs bind to high-affinity tyrosine kinase receptors that activate the intracellular Ras/Mapk signal transduction pathway, and in response the Fgf-feedback inhibitors Sprouty 2 (Spry2), Sprouty 4 (Spry4), Spred and Sef, and the ETS domain factors Erm and Pea3 (Furthauer et al., 2001; Raible and Brand, 2001; Lin et al., 2002; Furthauer et al., 2002; Raible and Brand, 2004; Sivak et al., 2005). To provide further evidence for a reception of Fgf signals by optic vesicle cells, we examined the activation of *spry4* as Fgf-target gene in domains overlapping and surrounding sites of Fgf gene expression. If the proposed Fgf8 signal from the telencephalon has a direct effect on NT eye patterning, Fgf-target genes should be expressed around the telencephalon, including the optic vesicle during the crucial patterning phase between the 5- and 10-somite stage.

We find that at the 5-somite stage *spry4* is co-expressed with *fgf8* in the telencephalon of wild-type embryos (Fig. 5A-D). Importantly, we find that *spry4* is expressed broader than *fgf8* and extends along the DV axis of the forebrain into the dorsal diencephalon and the proximal part of the evaginating optic vesicle. *Spry4* is also expressed in nasal placode precursors that surround the telencephalon at this stage (Fig. 5C,D). In *ace* embryos, the telencephalic and diencephalic expression of *spry4*, including the proximal optic vesicle, is strongly reduced, whereas the nasal placode precursors express *spry4* at normal levels (Fig. 5E,F). Thus, *spry4* is expressed and selectively dependent on *fgf8* in the diencephalon and proximal optic vesicle in the crucial phase for NT eye patterning, supporting the idea of an Fgf signal emanating from the telencephalon and reaching into the optic vesicle. Low-level *spry4* expression in the optic vesicle could explain the partial phenotype of *ace* mutants and argues for at least one other Fgf being involved in retinal NT patterning.

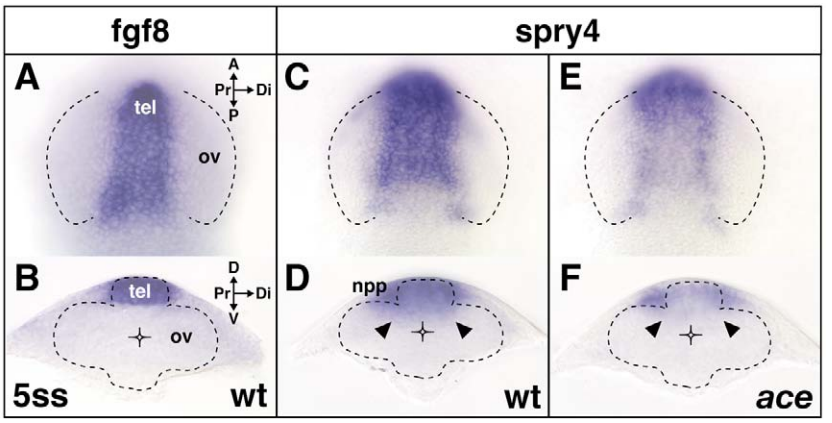

Fig. 5. Expression of *fgf8* and the Fgf-target gene *spry4,* during early eye development. At the 5-somite stage, *fgf8* and *spry4* are co-expressed in the telencephalon dorsal to the diencephalic evagination zone of the optic vesicles (A-D) in wild-type embryos. *spry4* expression extends from the telencephalon into the diencephalon, including the proximal future nasal part of the evaginating optic vesicle (arrowheads in D) and is found in the nasal placode precursor cells (npp) (D), surrounding the telencephalon at this stage. (E,F) In *ace*, telencephalic and diencephalic *spry4* expression is reduced (arrowheads in F), but expression in the nasal placode precursor cells is unaffected. Orientation of dorsal views (A,C,E,) indicated in A; orientation of transverse sections at a intermediate anterior-posterior level of the optic vesicle (B,D,F) indicated in B. A, anterior; P, posterior; Pr, proximal; Di, distal; D, dorsal; V, ventral; tel, telencephalon; ov, optic vesicle; npp, nasal placode precursors. Broken lines represent outlines of the optic vesicle (A,C,E,) and neural tube (B,D,F).

Fgf-dependent alterations of NT eye patterning result in topographic shifts of retinal axon mapping

To test (1) whether the effect of the Fgf signal on retinal patterning is irreversible during later development and (2) what the functional consequences of altered Efna/Eph expression in *ace* and Fgfr-inhibitor-treated embryos are, we studied the topographic projections of RGC axons to the midbrain optic tectum. For this purpose we grafted wild-type optic vesicles with or without prior Fgfr-inhibitor-treatment and optic vesicles from *ace* mutant embryos to wild-type hosts at the 10-somite stage (Fig. 6A). Anterograde co-labeling of the dorsotemporal (DT) and dorsonasal (DN) retinal quadrants with the lipophilic tracers DiI and DiO in wild-type control transplantations shows that DT and DN RGC axons form two spatially distinct termination zones (TZs) along the anterior-posterior axis of the ventral tectum, according to the NT

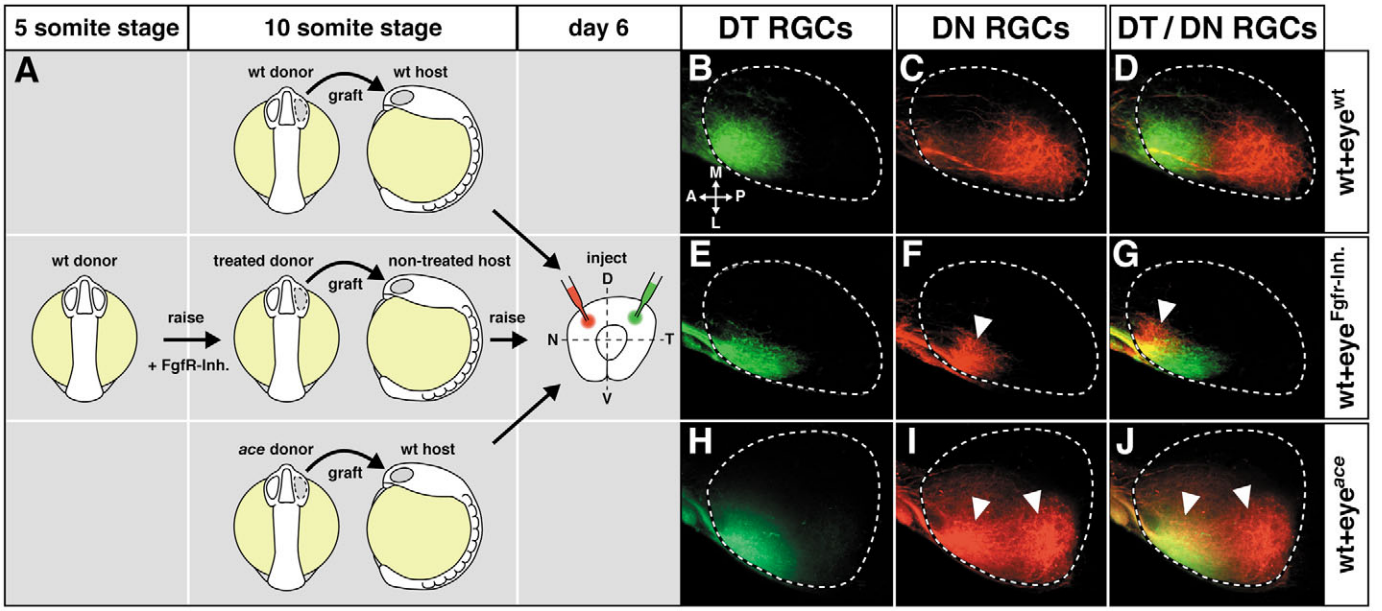

Fig. 6. Topographic shifts of tectal RGC projections from eyes with altered Fgf signaling. Retinotectal topography in chimeric larvae after transplantation of optic vesicles with Fgf-dependent alterations in NT patterning. (A) Transplantation scheme: optic vesicles were grafted from mock-treated wild-type donors to wild-type hosts (top), from Fgfr-inhibitor-treated donor embryos (treatment: 5- to 10-somite stage) to non-treated hosts (middle) and from *ace* donors to wild-type hosts (bottom) at the 10-somite stage. Chimeras were fixed at day 6 and retinal ganglion cell (RGC) axons anterogradely double-labeled by DiI (green) and DiO (red) in the dorsotemporal (DT) and dorsonasal (DN) quadrants. (B-D) In control transplantations, DT RGCs form an anterior termination zone (TZ) and DN RGCs form a posterior TZ that is non-overlapping and correct, according to their NT position in the retina (n=6/6). (E-G) Eyes from Fgfr-inhibitor-treated donor embryos display a full temporalization of RGC axon mapping: DT RGCs correctly terminate in an anterior TZ, while DN RGCs misproject to an ectopic anterior TZ (n=5/5). (H-J) Eyes from *ace* donor embryos display a partial temporalization of RGC axon mapping: DT RGCs correctly terminate anteriorly, while DN RGCs form a second, ectopic anterior TZ (n=5/6). White arrowheads indicate misprojections compared with wild type. Orientation of the tectum (dorsal views) as indicated in B. (B-J) Maximum-intensity projections of confocal image stacks. Broken outlines indicate the tectal neuropil. A, anterior; L, lateral; M, medial; P, posterior.

position of their somata in the retina (Fig. 6B-D). Wild-type larvae with an optic vesicle graft from an Fgfr-inhibitor-treated embryo show a pronounced topographic shift in the TZs of RGC axons: although the projection of DT RGC axons is unaltered and forms an anterior TZ, DN RGC axons display a completely 'temporalized projection behavior', terminating in an ectopic anterior TZ like the DT RGC axons (Fig. 6E-G). Wild-type larvae that received an optic vesicle graft from an *ace* embryo show an 'intermediate' RGC axon projection phenotype: the projections of DT RGC axons are unaltered and form an anterior TZ, but DN RGC axons form an ectopic anterior TZ in addition to the topographically correct posterior TZ (Fig. 6H-J).

These results demonstrate that the early defects in retinal NT patterning observed in the *ace* mutant and Fgfr-inhibitor-treated embryos produce corresponding topographic shifts in the later projection of RGC axons: partial temporalization of the nasal retina in *ace* and full temporalization upon Fgfr-inhibitor treatment. Furthermore, this shows that the alterations in eye patterning are irreversible after optic vesicle transplantation to wild-type host at the 10-somite stage and do not impair RGC differentiation. Consistent with the correct early DV patterning of the eye in the absence of *fgf8* and Fgfr signaling, we do not observe RGC axon misprojections along the DV axis of the tectum.

The NT axis of the prospective retina is established prior to the 7-somite stage

Finally, we asked whether any other or later signal derived from the forebrain or head of the embryo, apart from the Fgf signal, is required for retinal NT patterning. To achieve this, we grafted optic vesicles between the 5- and 7-somite stage ectopically onto the yolk cell, by slipping the graft into a pocket between the host epidermis and yolk cell membrane (Fig. 7A-C). Earlier transplants were not possible, because optic vesicle morphogenesis has just started at this stage. The transplantation spatially isolates the optic vesicle from the embryonic body proper and the above-described Fgf sources in the head region. Observation of live embryos shows that these heterotopic grafts integrate, grow and develop autonomously and ultimately form an ectopic, morphologically normal eye (Fig. 7D,E). At the 28 hour stage (16 hours post-transplantation) we tested NT gene expression, and find that both nasal expression of *efna5a* (n=5/7) and temporal *epha4b* expression (n=7/8) are correctly established and maintained in such grafts (Fig. 6F-I). This shows that the retina can undergo correct NT patterning in the absence of all signals from the forebrain or head after the 5- to 7-somite stage. Together with the results of the Fgfr inhibition experiments, this argues for an early Fgf signaling phase around the 5-somite stage that is sufficient to trigger autonomous NT eye patterning. The missing retinal pigment epithelium in the grafts at later stages of development (inset in Fig. 7E) is probably due to a lack of induction from the head mesenchyme in the ectopic situs (Fuhrmann et al., 2000).

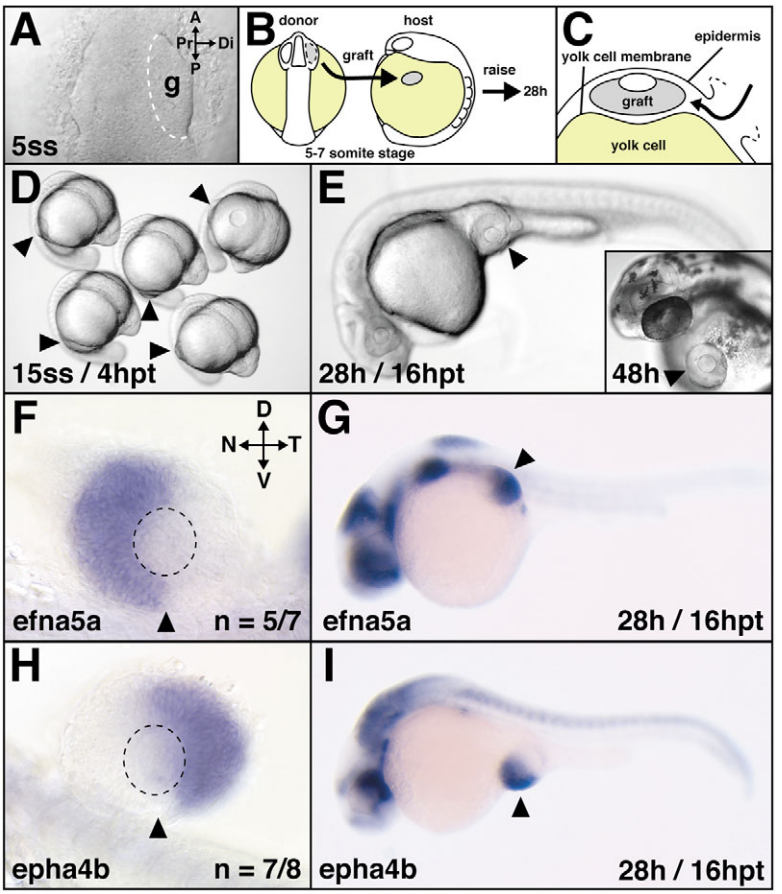

Fig. 7. Correct retinal NT patterning after heterotopic optic vesicle transplantation. (A-C) Transplantation scheme. At the 5- to 7-somite stage, optic vesicles were transplanted from the forebrain of donor embryos onto the yolk cell of hosts (B) by slipping the graft in between the locally-opened epidermis and the yolk cell membrane (C). A live image of the anterior neural keel (dorsal view) in shown in A, (D,E) Live host embryos: heterotopic grafts develop and differentiate on the yolk cell and form eyes of normal morphology. (F-I) Retinal NT patterning after heterotopic transplantation at 28 hours of development: in grafts, the nasal expression domain of *efna5a* (F) and the temporal expression domain of *epha4b* (H) are established and maintained normally in the ectopic situs (G,I) of the embryo. (F,H) Flat-mounts of dissected eyes, orientation as indicated in F. Arrowheads indicate the implantation site (D,E,G,I) and the ventralmost position of the eye (F,H). Broken outline in A indicates grafted tissue; in F,H it indicates the lens. A, anterior; P, posterior; g, graft; hpt, hours post-transplantation; D, dorsal; V, ventral; N, nasal; T, temporal; Pr, proximal; Di, distal.

Discussion

In this study, we have investigated the role of Fgf signaling in axial patterning of the prospective neural retina. We find that Fgf signaling determines positional cell identities along the NT axis of retina already at the time of optic vesicle formation (Fig. 8A). Temporally restricted inhibition of all Fgf receptor (Fgfr) signaling in embryos causes a complete 'nasal shift' of cell fates (Fig. 8C), while the 'nasal shift' observed in *fgf8*-mutant *ace* eyes is partial (Fig. 8B). The peak of sensitivity towards

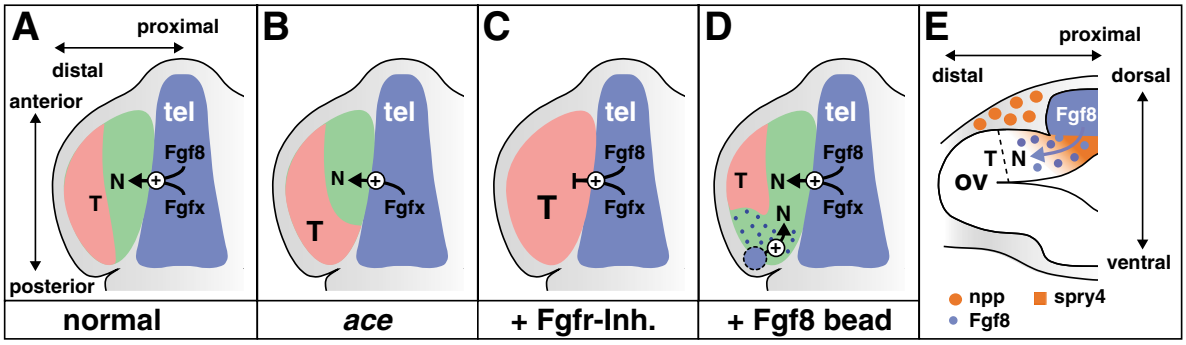

Fig. 8. Summary and model for Fgf-dependent retinal NT patterning. (A) In normal embryos, *fgf8* is expressed in the telencephalon (tel, in blue) at the 5-somite stage, medial and asymmetric to the evaginating optic vesicle (ov). The future nasal (N) retina (green) lies proximal to and the future temporal (T) retina (pink) lies distal to the telencephalic signaling source. Fgf8 from the telencephalon activates nasal cell fates in the proximal optic vesicle and thereby positions the NT boundary. (B) In *ace*, nasal fates are reduced and the retinal NT boundary shifts proximally/nasally owing to the lack of the Fgf8 signal, but an unknown Fgf signal (Fgfx) maintains some NT patterning. (C) Inactivation of all Fgf-receptor (Fgfr) signaling leads to a complete expansion of the temporal/distal cell fates throughout the retina at the expense of all nasal/proximal fates, as the telencephalic Fgf signal cannot activate the Fgf pathway in the optic vesicle. (D) Ectopic expression of Fgf8 by bead implantation locally induces nasal/proximal fates at the expense of temporal/distal fates. (E) Fgf8 activates *spry4* in the diencephalon and proximal optic vesicle, which indicates active Fgf signaling and a possible propagation route for Fgf8 along the dorsal-ventral axis of the forebrain and proximal-distal axis of the optic vesicle. npp, nasal placode precursors.

Fgfr-inhibition is between the 5- and 10-somite stage. Conversely, ectopic expression of Fgf8-protein induces a 'temporal shift' in NT patterning during this interval (Fig. 8D). Normal retinal DV patterning in the absence of Fgf signaling shows that this axis is determined independently of the NT axis. We therefore suggest that the crucial period for Fgf-dependent retinal patterning is between the 5- and 10-somite stage. During this period, *fgf8* expression is restricted to the telencephalon and neighboring the optic vesicle field; ectopically transplanted cells from this region can alter retinal NT patterning similar to Fgf8. Thus, Fgf8, emanating from the telencephalon probably acts as an extrinsic signal on eye patterning. Fgf8-dependent expression of the Fgf-target gene *spry4* around the telencephalon, in the dorsal diencephalon and in the optic vesicles further supports this hypothesis. Based on the local activation of *spry4*, it is most likely that Fgfs directly promote nasal cell fates. (Fig. 8E). Topographic misprojections of RGCs with Fgf-dependent shifts in NT patterning axons along the AP axis of the midbrain tectum underscore the irreversibility and functional relevance of these observations for later eye development and retinotectal mapping.

We conclude (1) that the period of optic vesicle evagination between 5- and 10-somite stage is the crucial phase for terminal, retinal NT patterning; (2) that Fgf8 acts together with at least one other, as yet unknown Fgf to determine this axis; and (3) that the source of the Fgf8 signal for NT patterning is the telencephalon. We thus suggest that the telencephalic precursors at this stage function as novel signaling center for axial patterning of the retina by signaling bilaterally into the evaginating optic vesicles. Interestingly, we find that in most experiments that the dorsonasal retina seems to be more sensitive to the Fgf signal than the ventronasal retina, which suggests a differential competence of primordium.

Combined Fgf signals including Fgf8 determine NT patterning of the prospective retina

We show that NT gene expression patterns in retinae compromised for Fgf signaling display a 'nasal shift' compared with the wild type (Fig. 8A-C). The complete 'nasal shift' in retinal polarity upon blocking of all Fgfr signaling, compared with the partial effect in the *ace* mutant and remnant *spry4* expression in *ace* mutant early optic vesicles, demonstrates the combinatorial nature of the Fgf signal (Fig. 8C). *fgf3* and *fgf24* have been previously described to function combinatorially with *fgf8* and are thus good candidates to be part of such a combinatorial signal (Leger and Brand, 2002; Walshe and Mason, 2003; Draper et al., 2003; Martinez-Morales et al., 2005). *fgf3* is strictly co-expressed with *fgf8* in the telencephalon at the 5-somite stage and there it regulates *spry4* expression together with *fgf8* (Fürthauer et al., 2001; Raible and Brand, 2001; Herzog et al., 2004). It thus could signal from the same source as *fgf8* during retinal patterning. *fgf24* is not expressed in the telencephalon, but in the mesenchymal precursor cells of the nasal placode, which are surrounding the anterior neural keel at the 5-somite stage, where *spry4* is also expressed but not dependent on Fgf8 (Whitlock and Westerfield, 2000). Previous studies have suggested the extraocular mesenchyme could act as source of extrinsic factors for optic vesicle differentiation (Fuhrmann et al., 2000). It is therefore possible that the *fgf24*-expressing precursors cells of the nasal placode act as an alternative source of Fgf during retinal NT patterning. Another candidate is the recently published *fgf17b*, which may be co-expressed with *fgf8* and *fgf3* in the telencephalon (Cao et al., 2004). Preliminary results with Fgf3 morpholinos (Leger and Brand, 2002) injected into *ace* mutant embryos suggest that Fgf8+Fgf3 cannot account for the signal (A.P. and M.B., unpublished). Further loss-of-function experiments will clarify the molecular nature of the Fgfs that function with Fgf8 in retinal NT patterning.

Gene expression along the retinal DV axis is not affected upon Fgf-dependent alterations in NT patterning. By experimentally interfering with Fgfs through gastrulation stages, two studies had suggested Fgfs to signal in parallel with Nodal, Hedgehog (Hh) and retinoic acid (RA) in DV eye

patterning (Take-uchi et al., 2003; Lupo et al., 2005). In addition, interactions between the DV and NT patterning mechanisms have been proposed (Huh et al., 1999; Mui et al., 2002; Sakuta et al., 2001; Koshiba-Takeuchi et al., 2000). Our results show that the crucial phase for Fgf-dependent retinal NT patterning is after gastrulation; interference with Fgf signaling during this time does not change DV patterning. The reduction in the dorsal expression domain of *tbx5*, that we observe in the *ace* mutant is restricted along the NT axis and does not affect the DV extent of the domain. This argues for the independence of the NT and DV eye patterning mechanisms.

The critical phase for NT patterning is at the onset of eye morphogenesis

The exact developmental timing of the events that lead to axial patterning of the retina has not been clearly resolved. Grafting studies in chick embryos suggest that the retinal NT axis is determined before HH stage 10-11 (10-13 somite stage) (Dutting and Meyer, 1995). Through combining loss- and gain-of-function analysis, we show that the crucial phase for Fgf-dependent NT patterning is between the 5- and 10-somite stage, when *fgf8* expression is clearly confined to the telencephalon and the optic vesicle has just started to evaginate from the diencephalon and is still connected along its full AP extent to the forebrain (Schmitt and Dowling, 1994). Fgfr inhibitor application during discrete developmental intervals was crucial for this observation, as a complete nasal shift in gene expression along the NT axis of the eye can only be induced by treatment between the 5- and 10-somite stage. Partial NT shifts induced by treatments directly before that stage, are most readily explained by persistence of the inhibitor. The importance of the phase between the 5- and 10-somite stage for eye patterning is independently supported by the reduced expression of the Fgf target *spry4* in the diencephalon and optic vesicle in *ace* mutant by the 5-somite stage, which indicates a non-autonomous requirement for Fgf8 in eye development at this early stage.

Interestingly, the *ace* mutant eye shows an extended responsiveness to Fgf8, beyond the early NT patterning phase, in rescue experiments. This is reminiscent of the observed plasticity in the midbrain-hindbrain region (Jaszai et al., 2003). But the observed, retained competence to respond to Fgf8 is limited as Fgfr-inhibitor treated and *ace* mutant eyes do not restore normal NT patterning, when transplanted into wild-type host brains beyond the 10-somite stage. Instead, patterning is terminally altered in the grafts, which is reflected by topographic RGC axon misprojections 5 days after transplantation. Thus, beyond the 10-somite stage, the endogenous patterning activity of Fgfs is not effective.

Previous studies have taken advantage of culturing optic vesicles or retinal explants to determine the influence of extrinsic signals on eye development (Pittack et al., 1997; Fuhrmann et al., 2000). Unexpectedly, our heterotopic transplantations of optic vesicles to the yolk cell at the 5- to 7-somite stage demonstrate that the inductive events prior to this stage are sufficient to drive correct NT patterning, autonomously in the absence of extrinsic cues from the forebrain/head. Taken together with our findings on the requirement for Fgfs, in particular Fgf8, during that period, we propose that a short pulse of Fgfs around the 5-somite stage triggers NT eye patterning, and the eye becomes independent of exogenous signal supply shortly thereafter.

Early Fgf-dependent eye patterning is required for topographic mapping of RGC axons

Because *epha4b* expression is confined to the temporal retina in normal zebrafish, its expansion could directly explain the misprojection of RGCs from the nasal retina of *ace* mutant and Fgfr-inhibitor treated eyes to an ectopic, anterior termination zone (TZ) by increasing the sensitivity of axons for repellent Efna-ligands expressed in gradients on the tectum (Brennan et al., 1997; Picker et al., 1999). Remarkably, nasal RGC axons from an *ace* mutant eye form an ectopic anterior TZ in addition to a normal posterior TZ, indicating a partial temporalization, in contrast to a full temporalization upon blocking of all Fgfr signaling. These duplicated TZs are similar to the observations made in mice with targeted deletions of Efna5, Efna2 and Efna5/Efna2 (Frisen et al., 1998; Feldheim et al., 2000). Consistent with normal gene expression along the DV axis of the retina, we do not find DV mapping defects of RGC axons from *ace* or Fgfr-inhibitor treated eyes. It has recently been shown that nasally expressed *foxg1* (*CBF1*) represses temporal and induces nasal gene expression, similar to the results that we obtain for Fgfs (Takahashi et al., 2003). It is thus possible that Fgf signaling acts upstream of the transcriptional regulator *foxg1*.

Propagation of the Fgf signal from a novel signaling center in the telencephalon

We propose that the telencephalon is the source of the Fgf8 signal that influences NT eye patterning. At the onset of optic vesicle evagination, between the 5- and 10-somite stage, the telencephalon is the only *fgf8* expression domain in the head region. Expression there coincides with the timing of the observed effects of Fgfs on NT eye patterning.

(1) Fgfr inhibitor treatments show that Fgf signaling is crucial between the 5- and 10-somite stage, and not required for NT patterning beyond the 10-somite stage, when Fgf8 starts to be expressed in the optic stalk and retina.

(2) Ectopic Fgf8 protein expression shows a restricted competence to induce NT patterning shifts between the 5- and 10-somite stage.

(3) Reduction of the graded expression of the Fgf target *spry4* in the dorsal diencephalon, including the proximal optic vesicle in the *ace* mutant at the 5-somite stage, shows active Fgf signaling in the region.

Although our loss-and gain-of-function experiments consistently show that Fgf8 influences retinal NT patterning, this effect could still be indirect and reflect a previously reported, autonomous requirement for Fgf8 during telencephalon development rather than a direct signal (Shanmugalingam et al., 2000; Walshe and Mason, 2003). However, the fact that (1) the Fgf target gene *spry4* is dependent on *fgf8* in the diencephalon and optic vesicle and (2) altered NT patterning after Fgf8-bead implantation support that Fgf8 itself is the signaling entity. As the simplest model, we thus favor a ‘trans-neuroepithelial’ propagation of the Fgf8 signal from the dorsal telencephalic source along the DV axis of the neural tube into the ventrally located diencephalon and the contiguous proximal-distal axis of the evaginating optic vesicle (Fig. 8E). Fate-mapping of cells in the optic vesicle at

the 10-somite stage shows that the proximal-distal and posterior-anterior axis of the vesicle match the NT and DV axis of the retina at later stages (Li et al., 2000). Thus, in the crucial patterning phase between the 5- and 10-somite stage, the NT axis of the prospective retina is perpendicular to the AP axis of the telencephalon, which therefore could function as an asymmetric Fgf source. Such a 'trans-neuroepithelial' Fgf8 distribution could well explain (1) the graded activation of *spyr4* in the diencephalon and optic vesicle, and (2) the Fgf-dependent induction of proximal/future nasal (*foxg1*- and *efna5a*-expressing) and suppression of distal/future temporal (*epha4b*-expressing) retinal cell fates. The similarity between the *ace* phenotype and the effects caused by partial Fgfr-inhibition suggests that the other Fgf(s) act via a similar mechanism, but analysis of further candidate Fgfs will be needed to determine whether the other molecular components of the combinatorial signal also emanate from the telencephalon.

Considering the role of Fgf expression at the midbrain-hindbrain boundary for tectal AP patterning (Lee et al., 1997; Picker et al., 1999), it is intriguing to find that Fgfs also determine eye patterning along the NT axis. Because both axes are matched in the topography of the retinotectal projection, it is tempting to speculate that this dual requirement reflects a common control mechanism for the positional code of cells in the source and target area of retinotectal map. If this were true, graded interference with Fgfs, common to source and target field, would create parallel shifts in axial patterning of eye and tectum. In evolutionary terms, this might confer 'robustness' to the map, because global fluctuations in Fgf signaling would result in coordinate changes of axial patterning of eye and tectum, which are compensated for each other in the retinotectal topography.

We thank Caroline Brennan and Uwe Drescher for reagents, and Carl-Philipp Heisenberg and Andrew Oates for comments on the manuscript. This work was supported by funds from the EU (Zf models), DFG SFB 655 and the Human Frontiers Science Program, and by the Max-Planck-Society to M.B.

Supplementary material

Supplementary material for this article is available at
http://dev.biologists.org/cgi/content/full/132/22/4951/DC1

References

Barbieri, A. M., Lupo, G., Bulfone, A., Andreazzoli, M., Mariani, M., Fougerousse, F., Consalez, G. G., Borsani, G., Beckmann, J. S., Barsacchi, G. et al. (1999). A homeobox gene, vax2, controls the patterning of the eye dorsal-ventral axis. *Proc. Natl. Acad. Sci. USA* **96**, 10729-10734.

Brand, M., Heisenberg, C. P., Jiang, Y. J., Beuchle, D., Lun, K., Furutani-Seiki, M., Granato, M., Haffter, P., Hammerschmidt, M., Kane, D. A. et al. (1996). Mutations in zebrafish genes affecting the formation of the boundary between midbrain and hindbrain. *Development* **123**, 179-190.

Brennan, C., Monschau, B., Lindberg, R., Guthrie, B., Drescher, U., Bonhoeffer, F. and Holder, N. (1997). Two Eph receptor tyrosine kinase ligands control axon growth and may be involved in the creation of the retinotectal map in the zebrafish. *Development* **124**, 655-664.

Cao, Y., Zhao, J., Sun, Z., Zhao, Z., Postlethwait, J. and Meng, A. (2004). fgf17b, a novel member of Fgf family, helps patterning zebrafish embryos. *Dev. Biol.* **271**, 130-143.

Cheng, H. J. and Flanagan, J. G. (1994). Identification and cloning of ELF-1, a developmentally expressed ligand for the Mek4 and Sek receptor tyrosine kinases. *Cell* **79**, 157-168.

Cheng, H. J., Nakamoto, M., Bergemann, A. D. and Flanagan, J. G. (1995). Complementary gradients in expression and binding of ELF-1 and Mek4 in development of the topographic retinotectal projection map. *Cell* **82**, 371-381.

Chow, R. L. and Lang, R. A. (2001). Early eye development in vertebrates. *Annu. Rev. Cell Dev. Biol.* **17**, 255-296.

Chuang, J. C. and Raymond, P. A. (2002). Embryonic origin of the eyes in teleost fish. *BioEssays* **24**, 519-529.

Crossley, P. H., Martinez, S. and Martin, G. R. (1996). Midbrain development induced by FGF8 in the chick embryo. *Nature* **380**, 66-68.

Deitcher, D. L., Fekete, D. M. and Cepko, C. L. (1994). Asymmetric expression of a novel homeobox gene in vertebrate sensory organs. *J. Neurosci.* **14**, 486-498.

Draper, B. W., Stock, D. W. and Kimmel, C. B. (2003). Zebrafish fgf24 functions with fgf8 to promote posterior mesodermal development. *Development* **130**, 4639-4654.

Drescher, U., Kremoser, C., Handwerker, C., Loschinger, J., Noda, M. and Bonhoeffer, F. (1995). In vitro guidance of retinal ganglion cell axons by RAGS, a 25 kDa tectal protein related to ligands for Eph receptor tyrosine kinases. *Cell* **82**, 359-370.

Dutting, D. and Meyer, S. U. (1995). Transplantations of the chick eye anlage reveal an early deterimination of nasotemporal polarity. *Int. J. Dev. Biol.* **39**, 921-931.

Feldheim, D. A., Kim, Y. I., Bergemann, A. D., Frisen, J., Barbacid, M. and Flanagan, J. G. (2000). Genetic analysis of ephrin-A2 and ephrin-A5 shows their requirement in multiple aspects of retinocollicular mapping. *Neuron* **25**, 563-574.

Flanagan, J. G. and Vanderhaeghen, P. (1998). The ephrins and Eph receptors in neural development. *Annu. Rev. Neurosci.* **21**, 309-345.

Friedman, G. C. and O'Leary, D. D. (1996). Retroviral misexpression of engrailed genes in the chick optic tectum perturbs the topographic targeting of retinal axons. *J. Neurosci.* **16**, 5498-5509.

Frisen, J., Yates, P. A., McLaughlin, T., Friedman, G. C., O'Leary, D. D. and Barbacid, M. (1998). Ephrin-A5 (AL-1/RAGS) is essential for proper retinal axon guidance and topographic mapping in the mammalian visual system. *Neuron* **20**, 235-243.

Fuhrmann, S., Levine, E. M. and Reh, T. A. (2000). Extraocular mesenchyme patterns the optic vesicle during early eye development in the embryonic chick. *Development* **127**, 4599-4609.

Furthauer, M., Reifers, F., Brand, M., Thisse, B. and Thisse, C. (2001). sprouty4 acts in vivo as a feedback-induced antagonist of FGF signaling in zebrafish. *Development* **128**, 2175-2186.

Furthauer, M., Lin, W., Ang, S. L., Thisse, B. and Thisse, C. (2002). Sef is a feedback-induced antagonist of Ras/MAPK-mediated FGF signalling. *Nat. Cell Biol.* **4**, 170-174.

Hatini, V., Tao, W. and Lai, E. (1994). Expression of winged helix genes, BF-1 and BF-2, define adjacent domains within the developing forebrain and retina. *J. Neurobiol.* **25**, 1293-1309.

Heisenberg, C. P., Brennan, C. and Wilson, S. W. (1999). Zebrafish aussicht mutant embryos exhibit widespread overexpression of ace (fgf8) and coincident defects in CNS development. *Development* **126**, 2129-2140.

Herzog, W., Sonntag, C., von der Hardt, S., Roehl, H. H., Varga, Z. M. and Hammerschmidt, M. (2004). Fgf3 signaling from the ventral diencephalon is required for early specification and subsequent survival of the zebrafish adenohypophysis. *Development* **131**, 3681-3692.

Huh, S., Hatini, V., Marcus, R. C., Li, S. C. and Lai, E. (1999). Dorsal-ventral patterning defects in the eye of BF-1-deficient mice associated with a restricted loss of shh expression. *Dev. Biol.* **211**, 53-63.

Hyatt, G. A., Schmitt, E. A., Marsh-Armstrong, N. R. and Dowling, J. E. (1992). Retinoic acid-induced duplication of the zebrafish retina. *Proc. Natl. Acad. Sci. USA* **89**, 8293-8297.

Hyatt, G. A., Schmitt, E. A., Marsh-Armstrong, N., McCaffery, P., Drager, U. C. and Dowling, J. E. (1996). Retinoic acid establishes ventral retinal characteristics. *Development* **122**, 195-204.

Itasaki, N. and Nakamura, H. (1996). A role for gradient en expression in positional specification on the optic tectum. *Neuron* **16**, 55-62.

Jaszai, J., Reifers, F., Picker, A., Langenberg, T. and Brand, M. (2003). Isthmus-to-midbrain transformation in the absence of midbrain-hindbrain organizer activity. *Development* **130**, 6611-6623.

Kastner, P., Grondona, J. M., Mark, M., Gansmuller, A., LeMeur, M., Decimo, D., Vonesch, J. L., Dolle, P. and Chambon, P. (1994). Genetic analysis of RXR alpha developmental function: convergence of RXR and RAR signaling pathways in heart and eye morphogenesis. *Cell* **78**, 987-1003.

Kimmel, C. B., Ballard, W. W., Kimmel, S. R., Ullmann, B. and Schilling, T. F. (1995). Stages of embryonic development of the zebrafish. *Dev. Dyn.* **203**, 253-310.

Koshiba-Takeuchi, K., Takeuchi, J. K., Matsumoto, K., Momose, T., Uno, K., Hoepker, V., Ogura, K., Takahashi, N., Nakamura, H., Yasuda, K. et al. (2000). Tbx5 and the retinotectum projection. *Science* **287**, 134-137.

Lee, S. M., Danielian, P. S., Fritzsch, B. and McMahon, A. P. (1997). Evidence that FGF8 signalling from the midbrain-hindbrain junction regulates growth and polarity in the developing midbrain. *Development* **124**, 959-969.

Leger, S. and Brand, M. (2002). Fgf8 and Fgf3 are required for zebrafish ear placode induction, maintenance and inner ear patterning. *Mech. Dev.* **119**, 91-108.

Li, Z., Joseph, N. M. and Easter, S. S., Jr (2000). The morphogenesis of the zebrafish eye, including a fate map of the optic vesicle. *Dev. Dyn.* **218**, 175-188.

Lin, W., Furthauer, M., Thisse, B., Thisse, C., Jing, N. and Ang, S. L. (2002). Cloning of the mouse Sef gene and comparative analysis of its expression with Fgf8 and Spry2 during embryogenesis. *Mech. Dev.* **113**, 163-168.

Logan, C., Wizenmann, A., Drescher, U., Monschau, B., Bonhoeffer, F. and Lumsden, A. (1996). Rostral optic tectum acquires caudal characteristics following ectopic engrailed expression. *Curr. Biol.* **6**, 1006-1014.

Lupo, G., Liu, Y., Qiu, R., Chandraratna, R. A., Barsacchi, G., He, R. Q. and Harris, W. A. (2005). Dorsoventral patterning of the Xenopus eye: a collaboration of Retinoid, Hedgehog and FGF receptor signaling. *Development* **132**, 1737-1748.

Marsh-Armstrong, N., McCaffery, P., Gilbert, W., Dowling, J. E. and Drager, U. C. (1994). Retinoic acid is necessary for development of the ventral retina in zebrafish. *Proc. Natl. Acad. Sci. USA* **91**, 7286-7290.

Martinez, S., Crossley, P. H., Cobos, I., Rubenstein, J. L. and Martin, G. R. (1999). FGF8 induces formation of an ectopic isthmic organizer and isthmocerebellar development via a repressive effect on Otx2 expression. *Development* **126**, 1189-1200.

Martinez-Morales, J. R., Del Bene, F., Nica, G., Hammerschmidt, M., Bovolenta, P. and Wittbrodt, J. (2005). Differentiation of the Vertebrate Retina Is Coordinated by an FGF Signaling Center. *Dev. Cell* **8**, 565-574.

McCabe, K. L., Gunther, E. C. and Reh, T. A. (1999). The development of the pattern of retinal ganglion cells in the chick retina: mechanisms that control differentiation. *Development* **126**, 5713-5724.

McLaughlin, T., Hindges, R. and O'Leary, D. D. (2003). Regulation of axial patterning of the retina and its topographic mapping in the brain. *Curr. Opin. Neurobiol.* **13**, 57-69.

Mohammadi, M., McMahon, G., Sun, L., Tang, C., Hirth, P., Yeh, B. K., Hubbard, S. R. and Schlessinger, J. (1997). Structures of the tyrosine kinase domain of fibroblast growth factor receptor in complex with inhibitors. *Science* **276**, 955-960.

Mui, S. H., Hindges, R., O'Leary, D. D., Lemke, G. and Bertuzzi, S. (2002). The homeodomain protein Vax2 patterns the dorsoventral and nasotemporal axes of the eye. *Development* **129**, 797-804.

Murali, D., Yoshikawa, S., Corrigan, R. R., Plas, D. J., Crair, M. C., Oliver, G., Lyons, K. M., Mishina, Y. and Furuta, Y. (2005). Distinct developmental programs require different levels of Bmp signaling during mouse retinal development. *Development* **132**, 913-923.

Nakamura, H. and Sugiyama, S. (2004). Polarity and laminar formation of the optic tectum in relation to retinal projection. *J. Neurobiol.* **59**, 48-56.

Peters, M. A. (2002). Patterning the neural retina. *Curr. Opin. Neurobiol.* **12**, 43-48.

Picker, A., Brennan, C., Reifers, F., Clarke, J. D., Holder, N. and Brand, M. (1999). Requirement for the zebrafish mid-hindbrain boundary in midbrain polarisation, mapping and confinement of the retinotectal projection. *Development* **126**, 2967-2978.

Pittack, C., Grunwald, G. B. and Reh, T. A. (1997). Fibroblast growth factors are necessary for neural retina but not pigmented epithelium differentiation in chick embryos. *Development* **124**, 805-816.

Raible, F. and Brand, M. (2001). Tight transcriptional control of the ETS domain factors Erm and Pea3 by Fgf signaling during early zebrafish development. *Mech. Dev.* **107**, 105-117.

Raible, F. and Brand, M. (2004). Divide et Impera – the midbrain-hindbrain boundary and its organizer. *Trends Neurosci.* **27**, 727-734.

Reifers, F., Bohli, H., Walsh, E. C., Crossley, P. H., Stainier, D. Y. and Brand, M. (1998). Fgf8 is mutated in zebrafish acerebellar (ace) mutants and is required for maintenance of midbrain-hindbrain boundary development and somitogenesis. *Development* **125**, 2381-2395.

Reifers, F., Walsh, E. C., Leger, S., Stainier, D. Y. and Brand, M. (2000). Induction and differentiation of the zebrafish heart requires fibroblast growth factor 8 (fgf8/acerebellar). *Development* **127**, 225-235.

Russell, C. (2003). The roles of Hedgehogs and Fibroblast Growth Factors in eye development and retinal cell rescue. *Vision Res.* **43**, 899-912.

Sakuta, H., Suzuki, R., Takahashi, H., Kato, A., Shintani, T., Iemura, S., Yamamoto, T. S., Ueno, N. and Noda, M. (2001). Ventroptin: a BMP-4 antagonist expressed in a double-gradient pattern in the retina. *Science* **293**, 111-115.

Sasagawa, S., Takabatake, T., Takabatake, Y., Muramatsu, T. and Takeshima, K. (2002). Axes establishment during eye morphogenesis in Xenopus by coordinate and antagonistic actions of BMP4, Shh, and RA. *Genesis* **33**, 86-96.

Schmitt, E. A. and Dowling, J. E. (1994). Early eye morphogenesis in the zebrafish, Brachydanio rerio. *J. Comp. Neurol.* **344**, 532-542.

Schulte, D. and Cepko, C. L. (2000). Two homeobox genes define the domain of EphA3 expression in the developing chick retina. *Development* **127**, 5033-5045.

Schulte, D., Furukawa, T., Peters, M. A., Kozak, C. A. and Cepko, C. L. (1999). Misexpression of the Emx-related homeobox genes cVax and mVax2 ventralizes the retina and perturbs the retinotectal map. *Neuron* **24**, 541-553.

Shanmugalingam, S., Houart, C., Picker, A., Reifers, F., Macdonald, R., Barth, A., Griffin, K., Brand, M. and Wilson, S. W. (2000). Ace/Fgf8 is required for forebrain commissure formation and patterning of the telencephalon. *Development* **127**, 2549-2561.

Sivak, J. M., Petersen, L. F. and Amaya, E. (2005). FGF signal interpretation is directed by Sprouty and Spred proteins during mesoderm formation. *Dev. Cell* **8**, 689-701.

Stadler, H. S. and Solursh, M. (1994). Characterization of the homeobox-containing gene GH6 identifies novel regions of homeobox gene expression in the developing chick embryo. *Dev. Biol.* **161**, 251-262.

Takahashi, H., Shintani, T., Sakuta, H. and Noda, M. (2003). CBF1 controls the retinotectal topographical map along the anteroposterior axis through multiple mechanisms. *Development* **130**, 5203-5215.

Take-uchi, M., Clarke, J. D. and Wilson, S. W. (2003). Hedgehog signalling maintains the optic stalk-retinal interface through the regulation of Vax gene activity. *Development* **130**, 955-968.

Uemonsa, T., Sakagami, K., Yasuda, K. and Araki, M. (2002). Development of dorsal-ventral polarity in the optic vesicle and its presumptive role in eye morphogenesis as shown by embryonic transplantation and in ovo explant culturing. *Dev. Biol.* **248**, 319-330.

Walshe, J. and Mason, I. (2003). Unique and combinatorial functions of Fgf3 and Fgf8 during zebrafish forebrain development. *Development* **130**, 4337-4349.

Westerfield, M. (2000). The zebrafish book. A guide for the laboratory use of zebrafish (Danio rerio). Eugene: University of Oregon Press.

Whitlock, K. E. and Westerfield, M. (2000). The olfactory placodes of the zebrafish form by convergence of cellular fields at the edge of the neural plate. *Development* **127**, 3645-3653.

Yang, X. J. (2004). Roles of cell-extrinsic growth factors in vertebrate eye pattern formation and retinogenesis. *Semin. Cell Dev. Biol.* **15**, 91-103.

Yuasa, J., Hirano, S., Yamagata, M. and Noda, M. (1996). Visual projection map specified by topographic expression of transcription factors in the retina. *Nature* **382**, 632-635.